Supporting Information

for

Mechano-responsive supramolecular metal-organic framework (supraMOF) gel material rich with ZIF-8 nanoplates

*Abhijeet K. Chaudhari and Jin-Chong Tan**
Multifunctional Materials & Composites (MMC) Laboratory,
Department of Engineering Science, University of Oxford,
Parks Road, Oxford OX1 3PJ, U.K.

**jin-chong.tan@eng.ox.ac.uk*

Table of Contents

1 Experimental Methods

1.1 Synthesis of ZIF-8 supraMOF gel material

12.0 mmol of 2-methylimidazole (mIm) was dissolved and deprotonated in 3 mL of *N*, *N*-dimethylformamide (DMF), followed by addition of 12.0 mmol of trimethylamine (NEt_3) into it. Another solution was prepared by dissolving 3.0 mmol of $Zn(NO_3)_2$ solution in another 3 mL of DMF. The former solution was then combined with the latter solution, they immediately reacted to form a gel network in solution phase. This solution containing gel product was then sonicated for 5 seconds which yielded a uniform and stable supraMOF gel material.

1.2 Critical concentration of gel

We performed reactions by maintaining the same volume of solvent, but varying the ratio of the metal : linker reactants. Table S1 lists the concentrations used to determine the minimum concentration required to obtain gelation. The gel/sol products are shown in Figure S1. It was established from the series of reactions that, the minimum ratio of Zn(II) : mIm required to achieve gelation is 1 : ~2.6. We note that no gelation occurred when less than 1 mmol of Zn(II) was used.

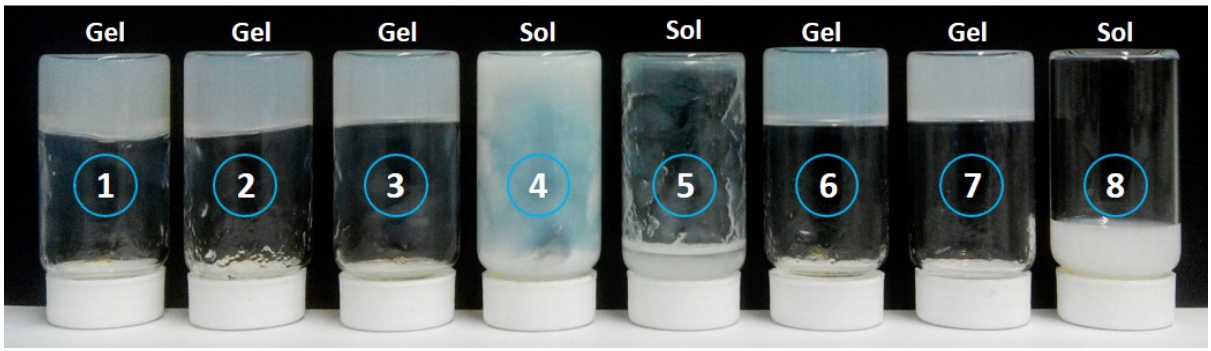

Figure S1. Products obtained from reactions employing different concentrations as tabulated in Table S1, showing stable gelation or no gelation (sol).

Table S1. Reactions performed using different concentrations of metal ions and organic linkers for determining the minimum required concentration for gel formation. In all reactions, NEt_3 was used in the same proportion to that of mIm for deprotonation of single protonic site. Refer to figure S1 to see the products obtained from reactions 1 to 8.

Sample	$Zn(NO_3)_2$ in 3 ml DMF	mIm in 3 ml DMF	Gel/Sol
1	3.0 mmol	12.0 mmol	Gel
2	3.0 mmol	10.0 mmol	Gel
3	3.0 mmol	8.0 mmol	Gel
4	3.0 mmol	6.0 mmol	Sol
5	3.0 mmol	3.0 mmol	Sol
6	2.0 mmol	8.0 mmol	Gel
7	1.0 mmol	4.0 mmol	Gel
8	0.5 mmol	2.0 mmol	Sol

1.3 Lower-symmetry ZIF-8 nanoplates extracted from supraMOF gel

The supraMOF gel material was disintegrated by adding 50 mL of additional DMF and then sonicated for 10 minutes. It produced a solution containing the dispersed white powder particles of ZIF-8 nanoplates. This colloidal suspension was centrifuged at 8000 rpm for 5 minutes, to isolate a white compound at the bottom of the tube. This precipitated product was then washed thoroughly using 50 mL of methanol twice and 50 ml of acetone later. At each washing step, compound in centrifuge tube was sonicated for 10 minutes before centrifuging. After washing, the compound was dried under vacuum at 110 °C. This final drying step will transform the powder precipitate by reconstituting the ZIF-8 nanoplates into a monolith.

1.4 Synthesis of conventional ZIF-8

2-methylimidazole (12.0 mmol) and $Zn(NO_3)_2$ (3.0 mmol) were dissolved together in 50 mL of methanol and stirred till white product precipitates at room temperature. The obtained product was thoroughly washed with plenty of methanol, centrifuged, and finally dried under vacuum at 100 °C.

1.5 Materials characterisation

Rheological measurements on the supraMOF gel sample were performed using Physica MCR-301 (Anton Paar) Rheometer equipped with a temperature-controlled basal plate. Parallel plate was used throughout all studies with a 2-mm gap between the basal and the top plates. Already synthesised gel was coated on glass substrate for investigation under the Carl Zeiss EVO LS15 scanning electron microscope (SEM). Sample was coated by thin layer of gold using SC7620 Polaron sputter coater (Quorum Technologies) before subjecting it to SEM. Powder X-ray diffraction (PXRD) study was performed on dry powder samples using Rigaku Miniflex diffractometer with a Cu Kα source (1.541 Å); diffraction data was collected between the 2θ of 2° to 30°, at a speed of 1° min^{-1} with 0.01° step size. AFM characterisation was performed using the Veeco Dimension 3100, under the standard tapping mode and a silicon tip. Thermogravimetric analysis (TGA) was performed on the TA Instrument Q50 by applying a heating rate of 20 °C min^{-1} from 30-500 °C.

2 Dynamic strain sweep rheology measurements

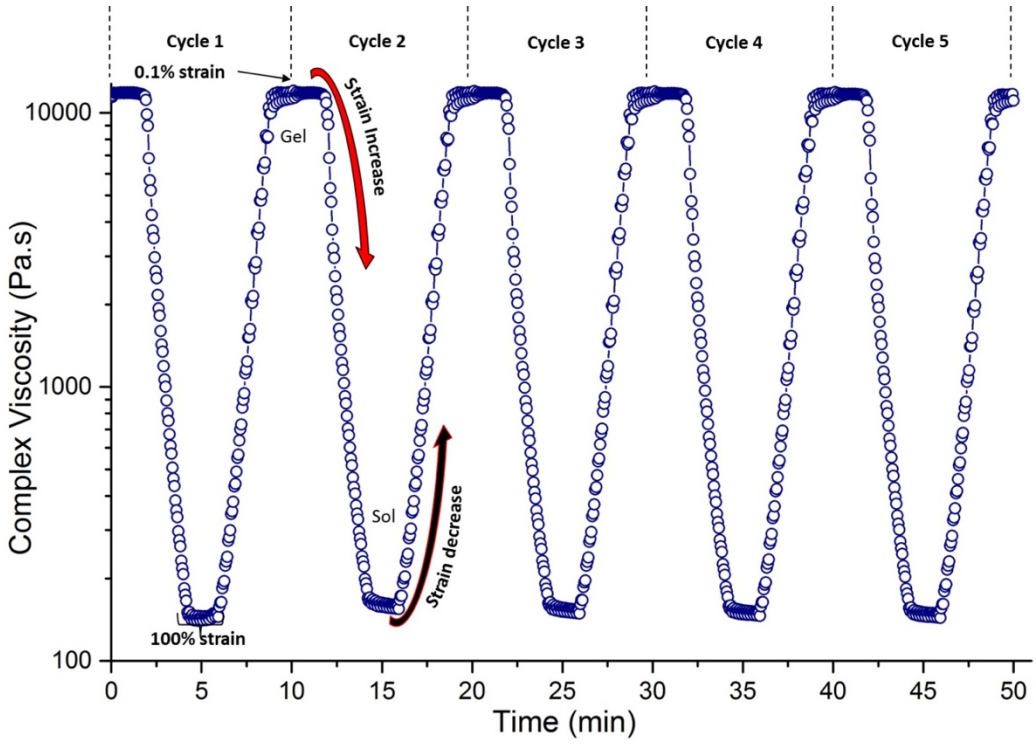

Figure S2. Complex viscosity measurement of ZIF-8 supraMOF gel sample for consecutive five cycles with dynamic strain sweep between a shear strain of 0.1% to 100%. Removal of strain recovers viscosity of gel sample confirming the reversible phase change of material switching between the sol ⇌ gel phases under cyclic mechanical deformation. Each cycle consists of: 250 sec from 0.1% to 100% strain causing gel → sol, hold for 100 sec, 250 sec from 100% to 0.1% strain causing sol → gel, hold for 100 sec, then repeat.

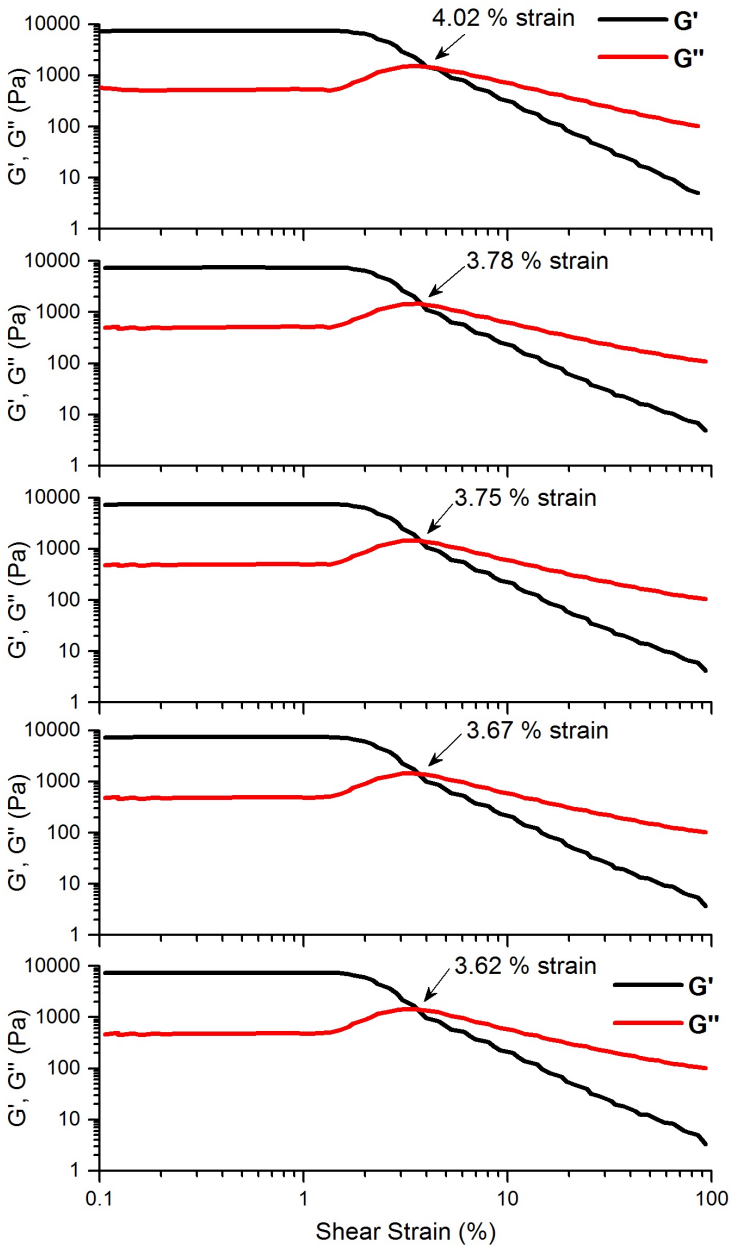

Figure S3. Dynamic strain sweep measurements for five consecutive shear strain cycles of 0.1% to 100%, corresponding to the data in Fig.1(c) in main manuscript. The yield points (in %) were established at the intercepts of the *G*' and *G*" data.

3 Scanning electron microscopy (SEM) images

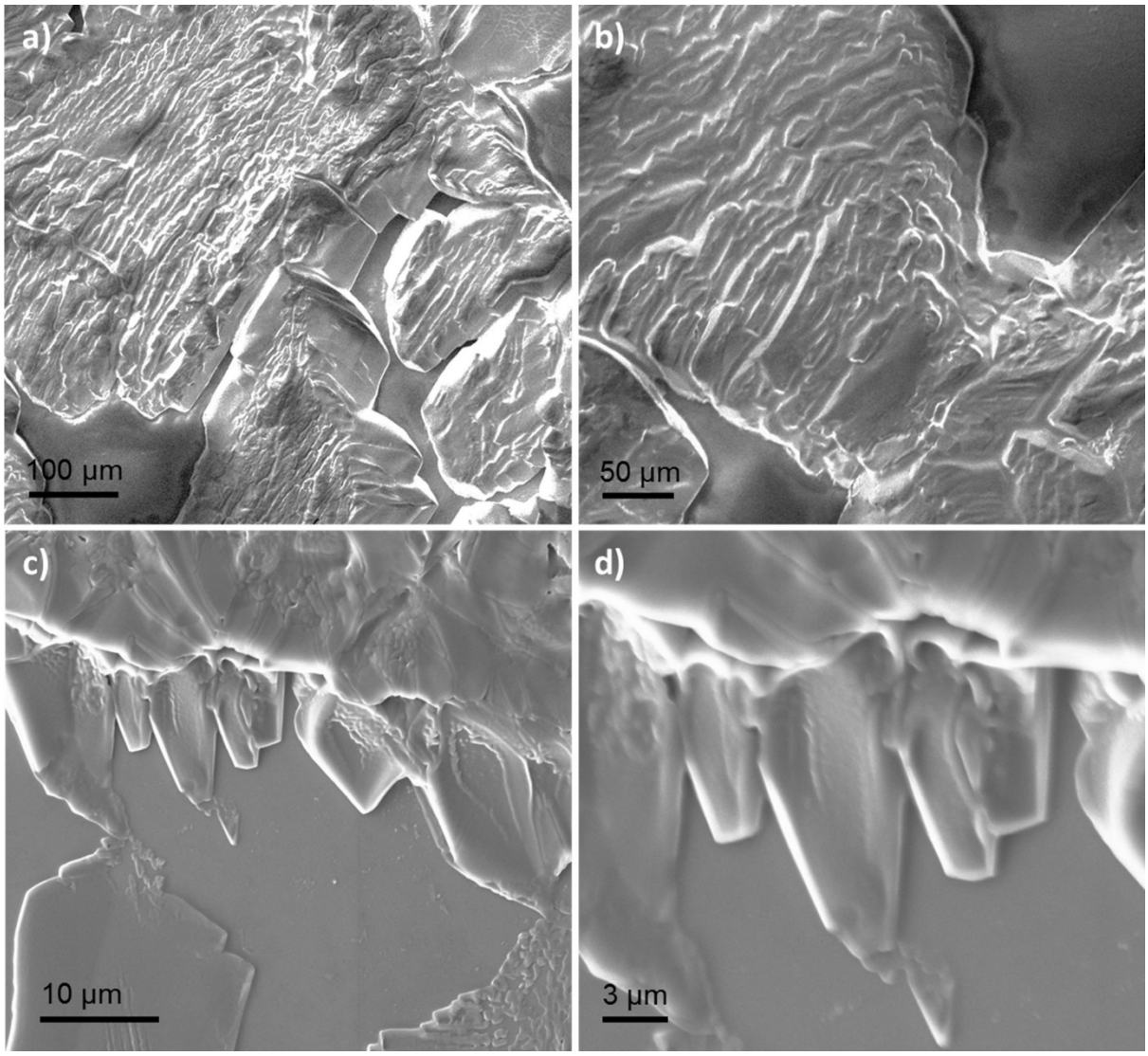

Figure S4. SEM images of the supraMOF gel sample coated onto glass substrates. Micrographs taken at different magnifications revealing the underlying 2D morphology of ZIF-8 nanoplates (see §4 and §5).

4 Transmission electron microscopy (TEM) images

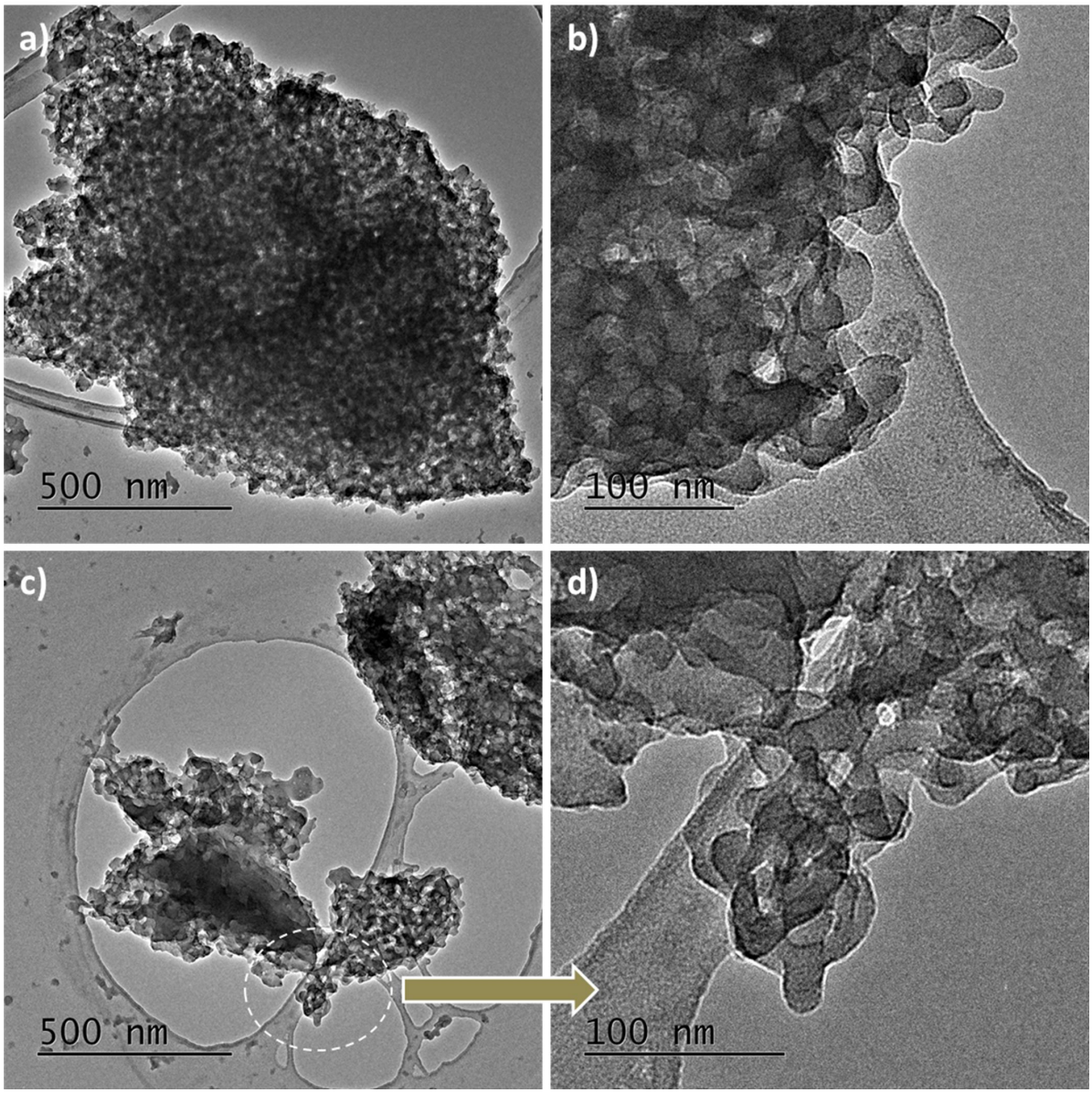

Figure S5. TEM images of reconstituted nanoplates extracted from the supraMOF gel (sample obtained from the dried ZIF-8 monolith). Aggregation can be seen even after long sonication of ground monolith sample for 4 hr in methanol. Panels (b) and (d) are zoomed areas around the edges of the aggregated material showing several thin 2D morphologies intertwined with each other.

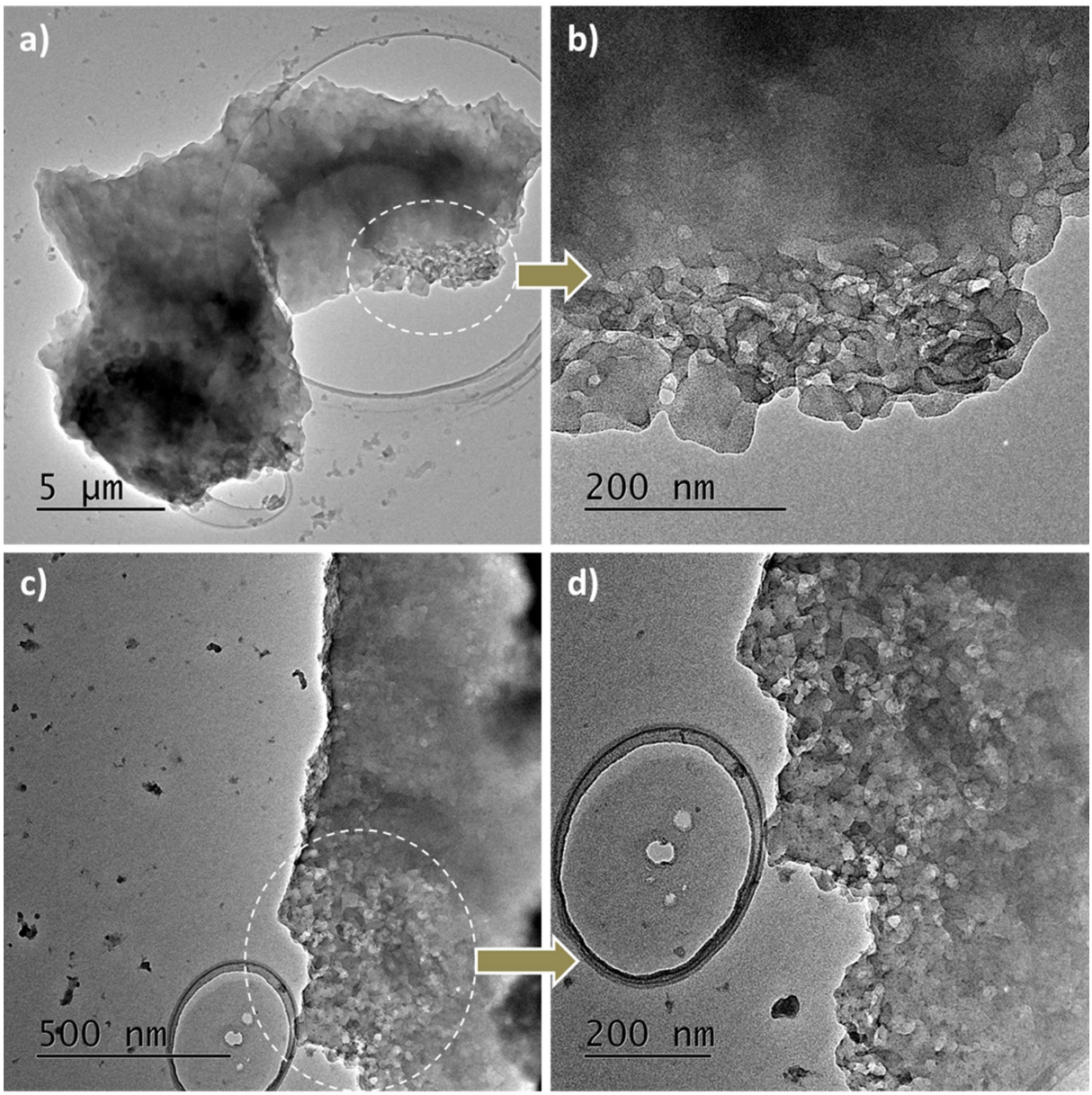

Figure S6. TEM images of nanoplate samples obtained from a dried ZIF-8 monolith revealing an aggregation of thin 2D morphology. Panels (b) and (d) are zoomed areas to show the intertwined thin nanosheets which are making up the larger micron-sized aggregate in panel (a).

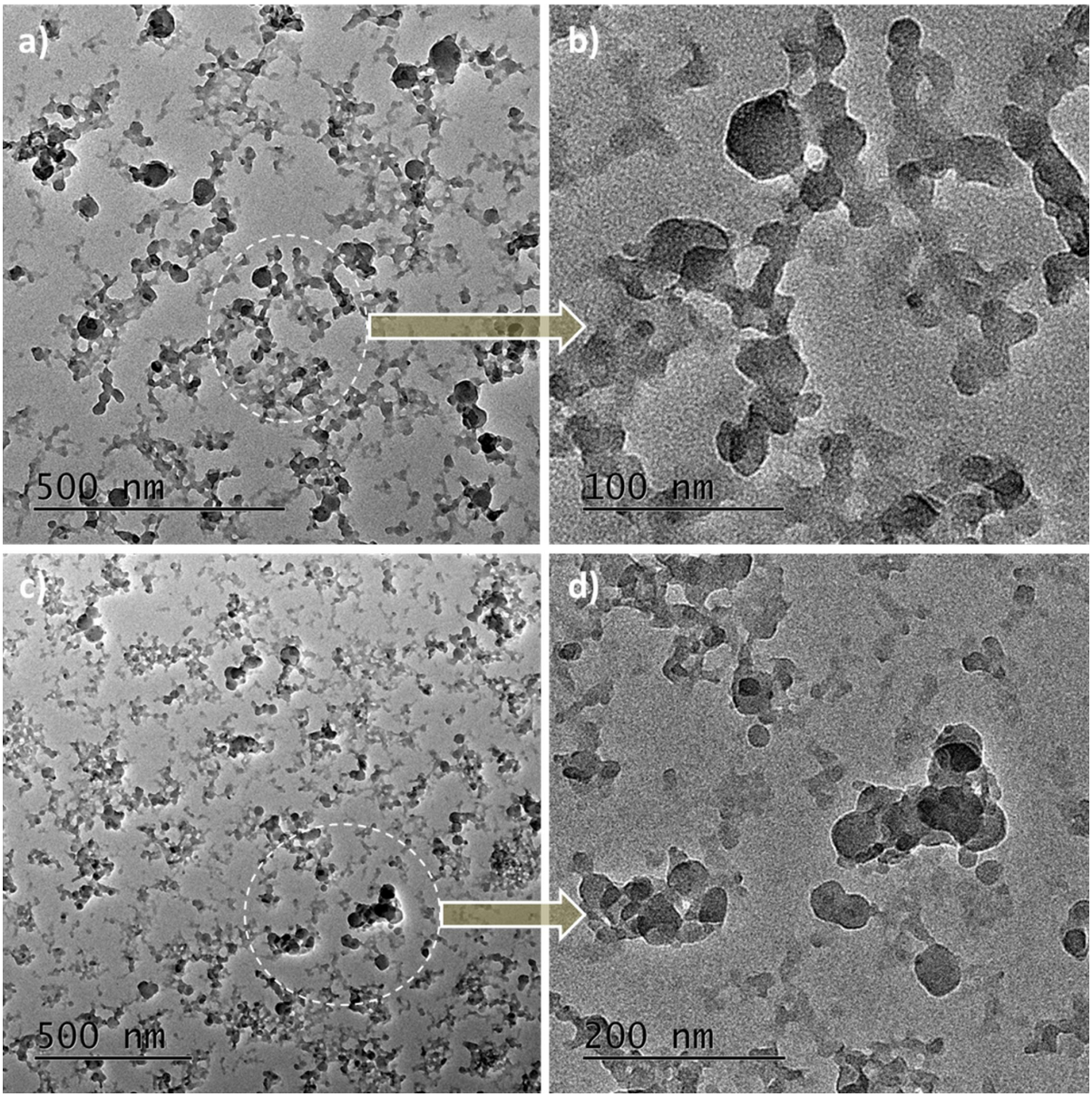

Figure S7. TEM images of as-synthesized ZIF-8 sample showing isolated nanoplates extracted from the supraMOF gel phase before subjecting to vacuum drying. Wet washed sample can be easily dispersed in methanol and ideal for imaging purposes in order to understand detailed features of the material. Very thin nanosheets of a few 10's of nm dimension can be seen in (b) and (d).

5 Atomic force microscopy (AFM) and nanoplate thickness characterisation

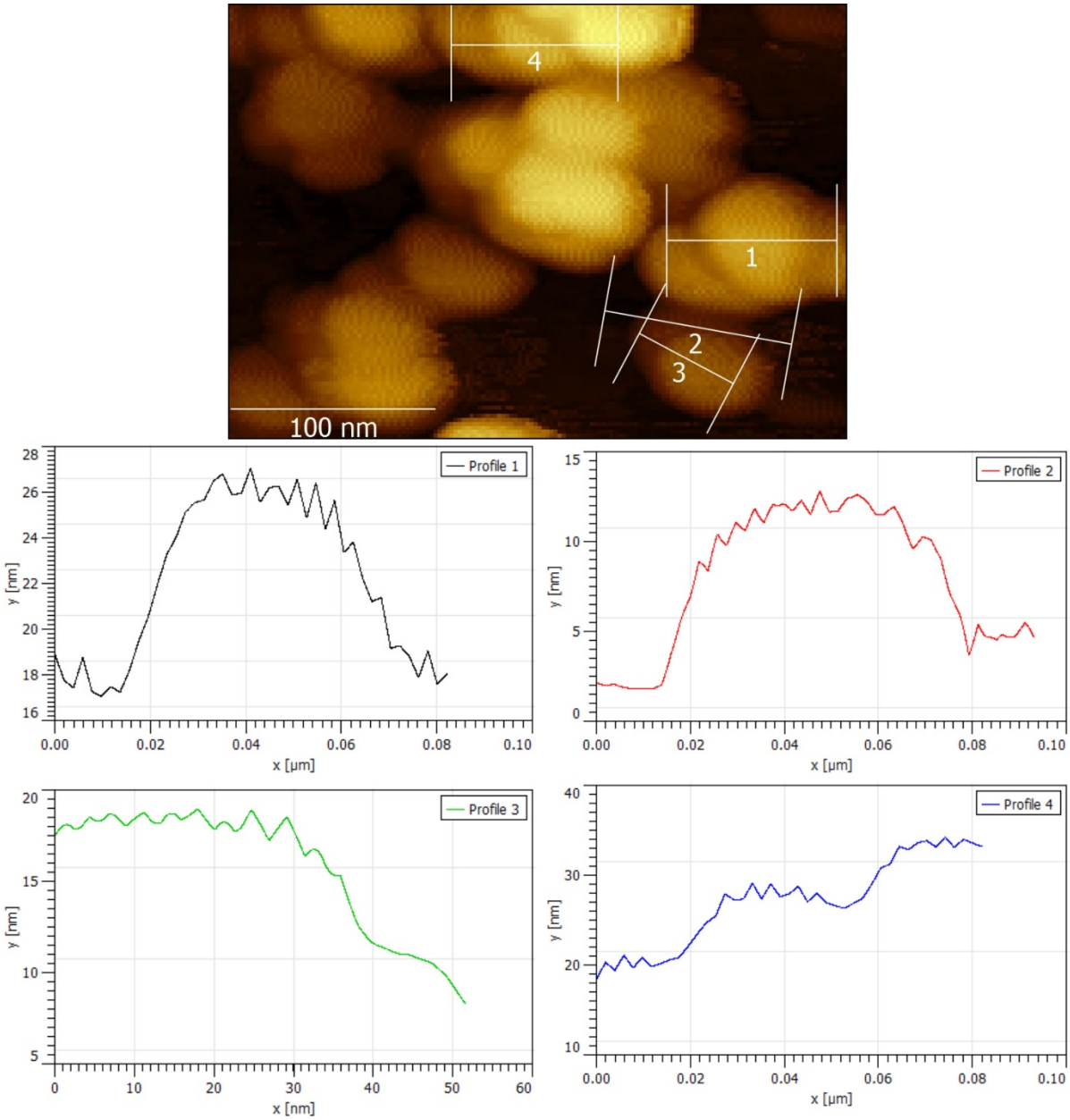

Figure S8. Atomic force microscopy (AFM) images for determining the nanoplate thickness (Table S2). The thickness profiles correspond to the locations marked in the height topography image at the top.

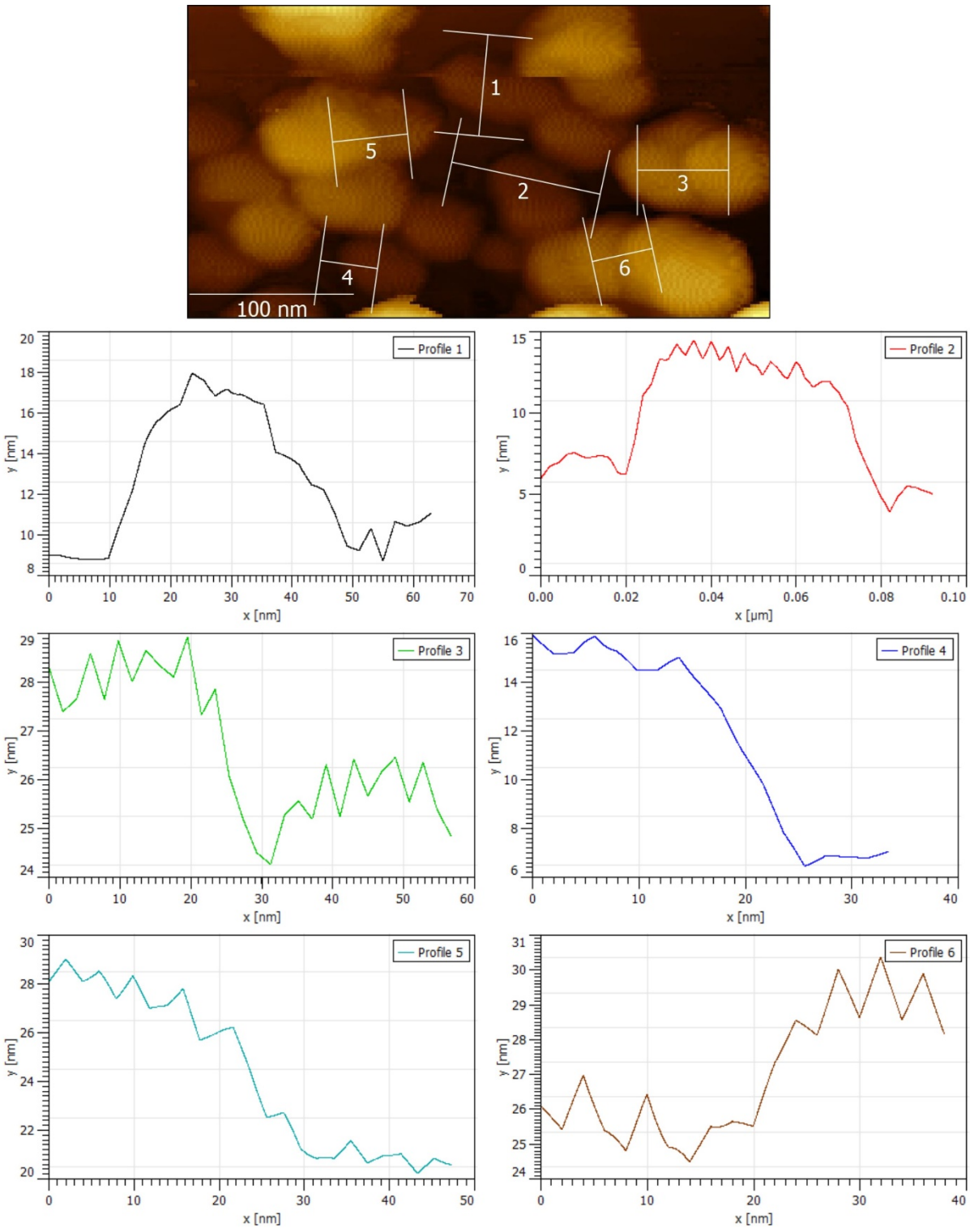

Figure S9. Nanoplate thickness profiles using AFM.

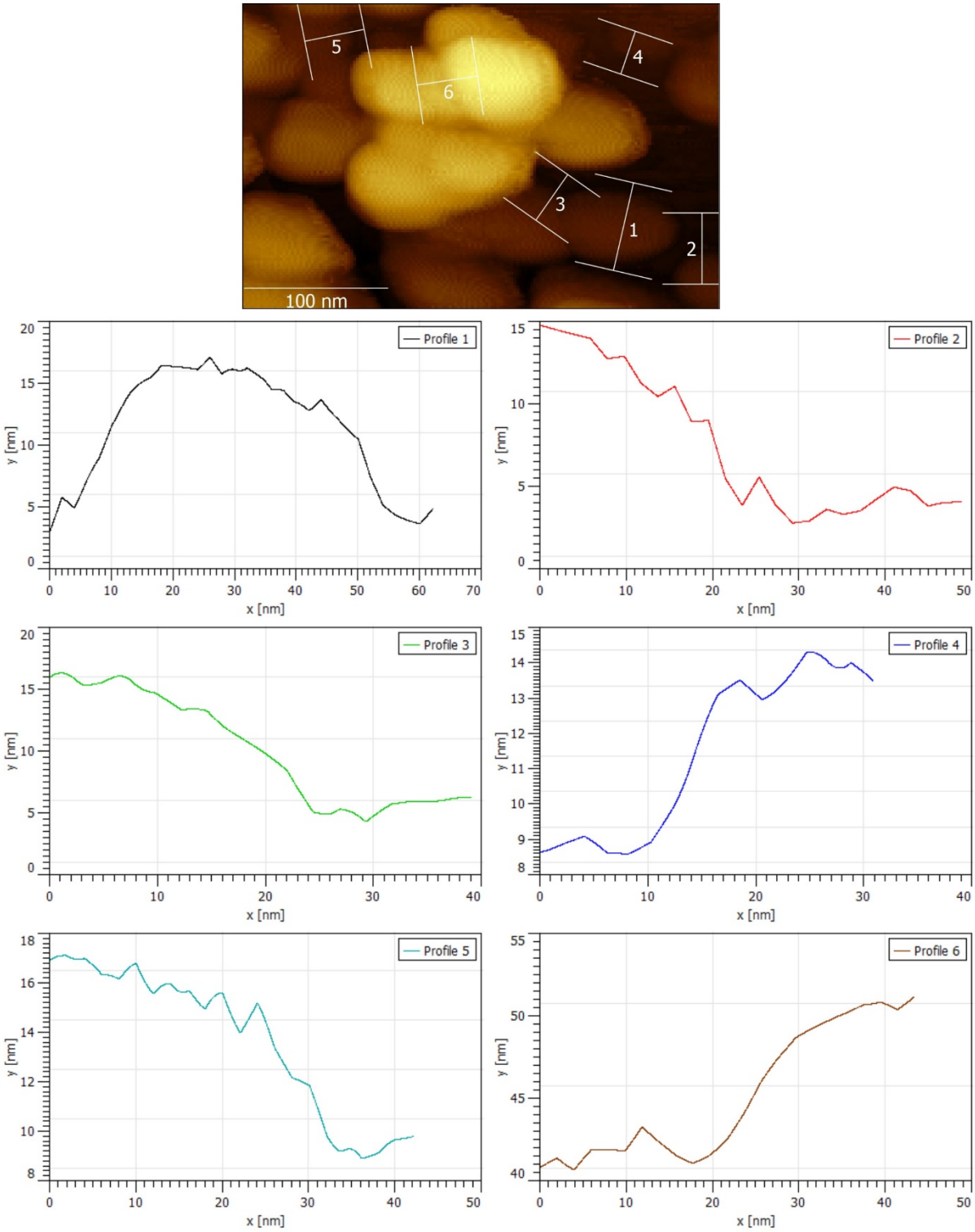

Figure S10. Nanoplate thickness profiles using AFM.

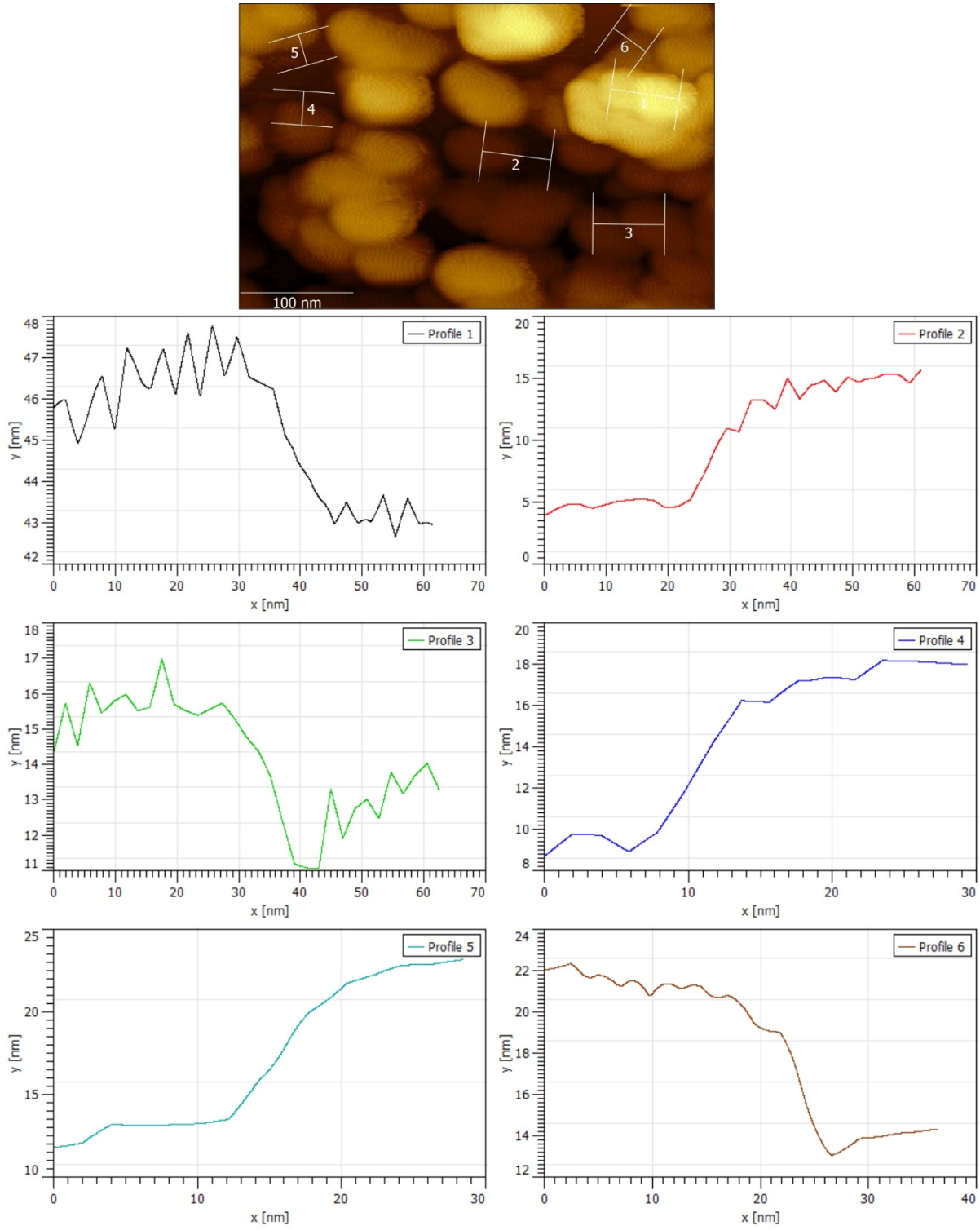

Figure S11. Nanoplate thickness profiles using AFM.

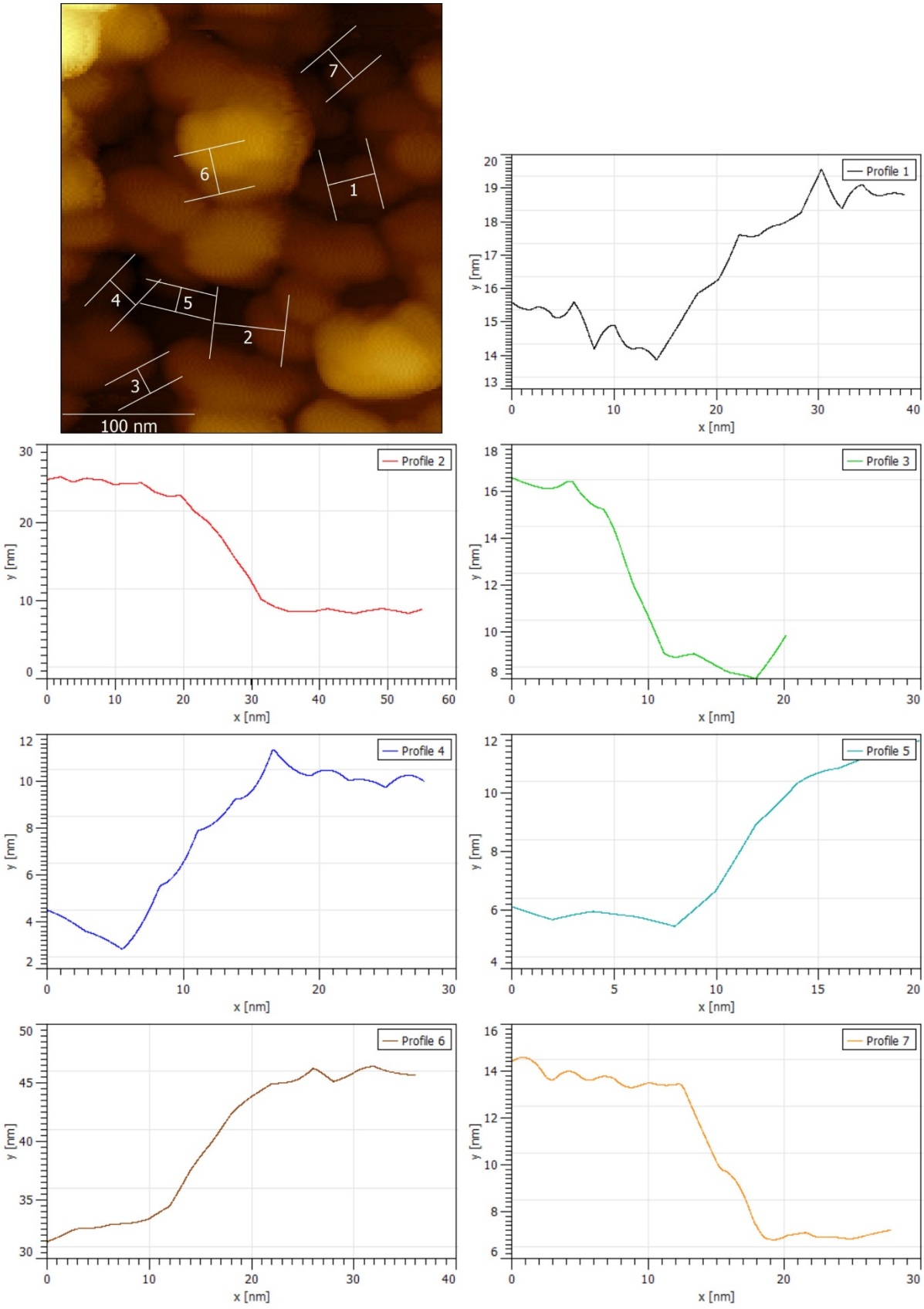

Figure S12. Nanoplate thickness profiles using AFM.

Table S2: Quantification of the nanoplate thickness using the AFM height topography data. Based on 35 sampling points, we determined the thickness to be 9.3 ± 3.8 nm.

Figure No.	Profile #	Thickness (nm)	Mean ± standard deviation (nm) calculated from 35 samples
S7	1	25.6-17.2=8.4	9.26 ± 3.77 nm
	2	14-4=10	
	3	18-11=7	
	4	1)= 28-20=8	
		2)= 34-28=6	
S8	1	17-9=8	
	2	13-6=7	
	3	28.4-24.3=4.1	
	4	15.4-6.8=8.6	
	5	28-20.4=7.6	
	6	29.5-25.8=3.7	
S9	1	16-3=13	
	2	15-3=12	
	3	16-4=12	
	4	14-8.5=5.5	
	5	17-8.6=8.4	
	6	52-40=12	
S10	1	47-43=4	
	2	15-4=11	
	3	16-11=5	
	4	18-9=9	
	5	23-13=10	
	6	22-14=8	
S11	1	19-14=5	
	2	26-8=18	
	3	16.6-8=8.6	
	4	10.6-3=7.6	
	5	11-5.6=5.4	
	6	46-32=14	
	7	14-6.8=7.2	
Fig.2 (c-d) (in the main manuscript)	1	13	
	2	11	
	3	11	
	4	18	
	5	16	

6 X-ray determination of crystal structure from Pawley refinement

Table S3. Changes in the unit cell parameters of the (distorted) ZIF-8 structure due to high concentration reaction and encapsulation of the Perylene guest within the pores of ZIF-8.

Compound	ZIF-8 reported by Yaghi et *al*.[1]	Nanoplates of ZIF-8
Crystal System	Cubic	Triclinic
Space Group	I-4 3 m	P1
X-ray Source	MoKα	CuKα
λ [Å]	0.71073	1.5418
Refinement Range of 2θ [°]	-	5 to 30
a [Å]	16.9910(12)	17.46
b (Å]	16.9910(12)	17.12
c [Å]	16.9910(12)	16.95
α [°]	90	89.01
β [°]	90	89.50
γ [°]	90	88.19
Peak Profile	-	Pseudo-Voigt
R factor	0.0314 (R1)	0.0642 (R_{wp})
Structure Solution Method	Single Crystal	Powder Refinement
Software	SHELXTL' 97	Reflex (Material Studio)

7 Thermogravimetric analysis (TGA)

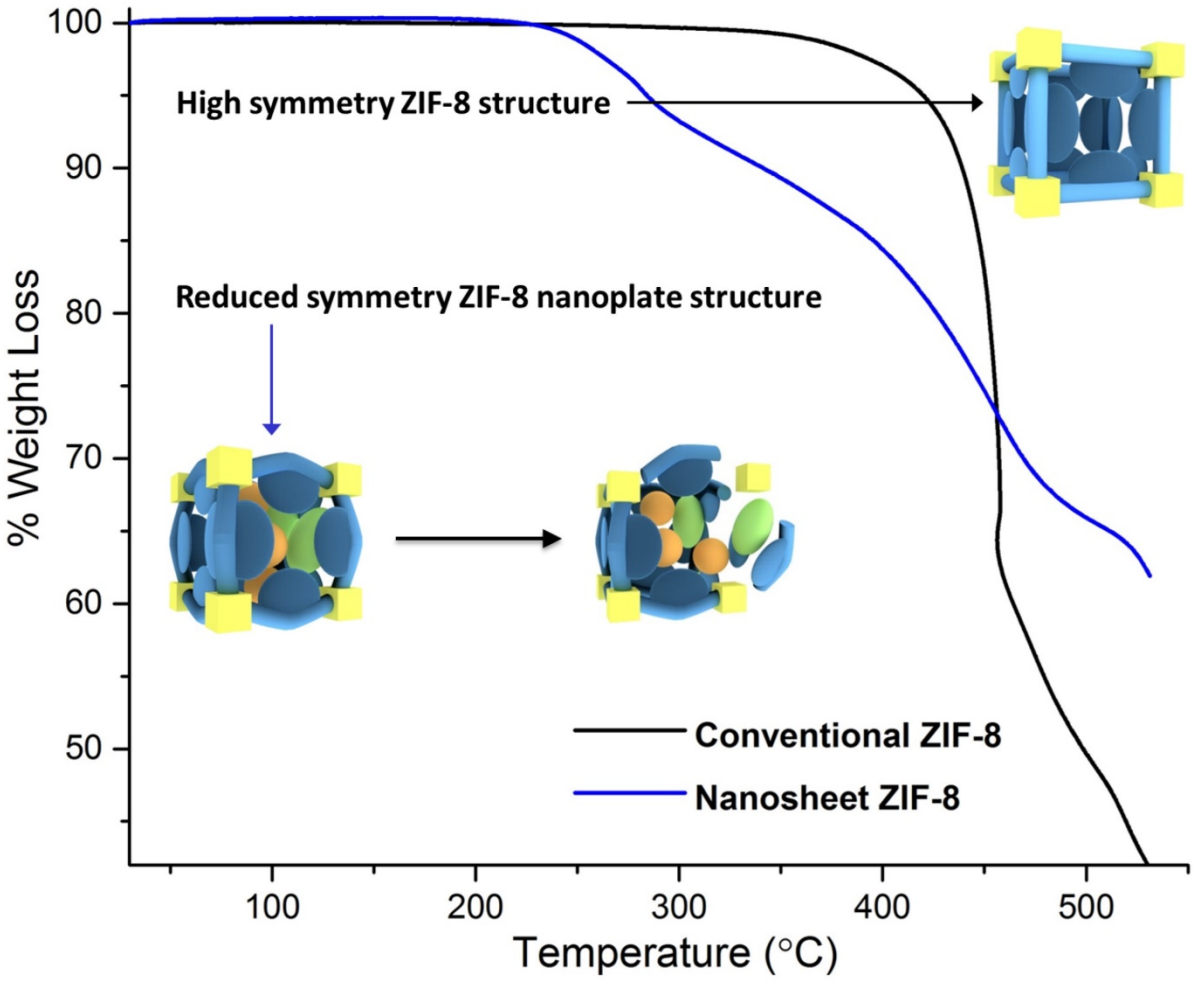

Figure S13. Comparison of the thermal stability of two different phases of ZIF-8, (conventional) high-symmetry cubic framework and low-symmetry triclinic framework found in ZIF-8 nanoplates. Due to high-concentration reaction (HCR) synthesis, occluded guest species inside the distorted ZIF-8 nanoplates will induce additional strains from inside the framework, causing it to collapse at a lower decomposition temperature versus the conventional ZIF-8 structure.

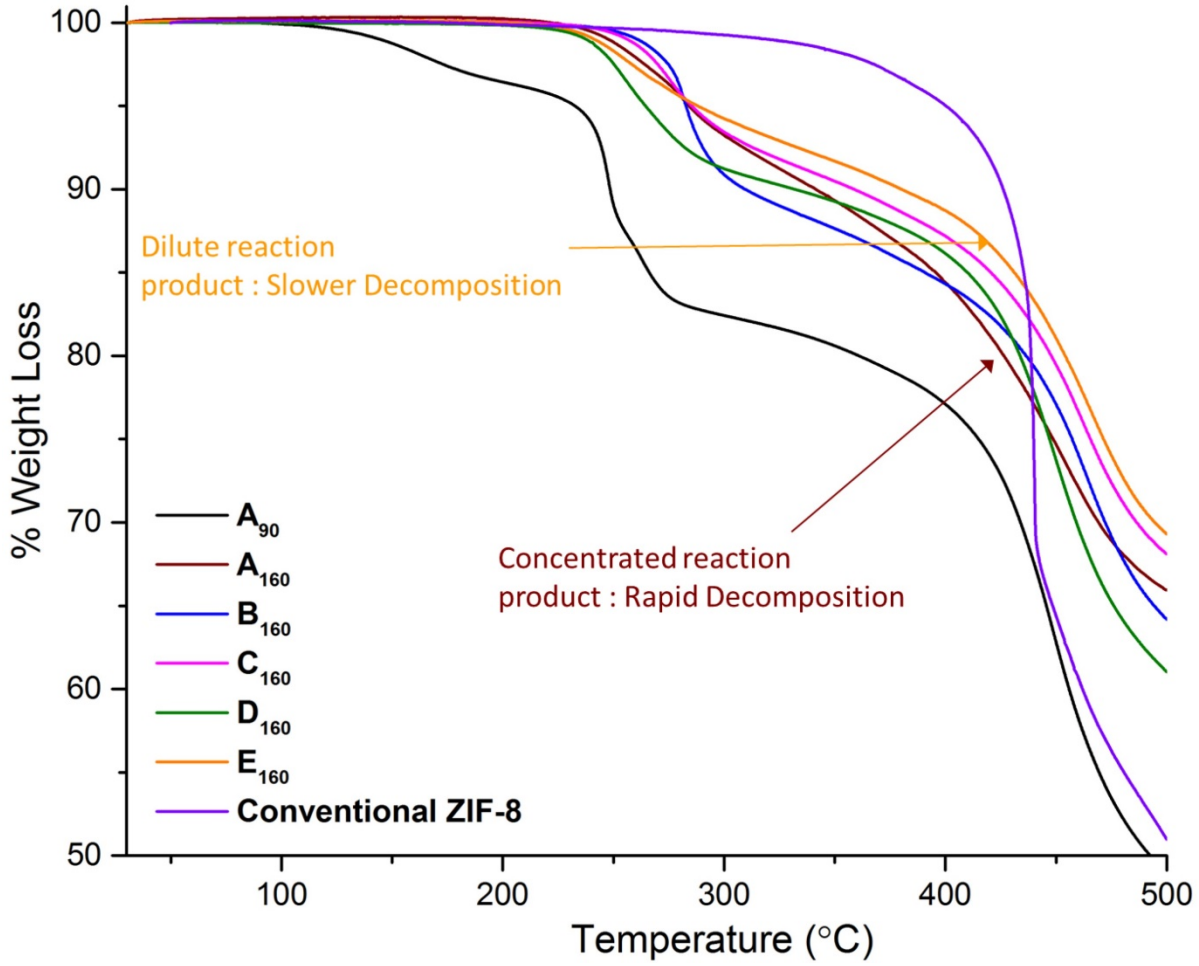

Figure S14. TGA of a series of compounds obtained ranging from concentrated to dilute reaction conditions (A→E), in accordance with Table 1 presented in the main manuscript. Comparing A_{90} to A_{160} (both extracted from supraMOF gel), it can be seen that by simply drying the same product "A" at a higher temperature of 160°C prior to TGA could enhance its thermal stability up to ~250°C, suggesting the removal of occluded guests (e.g. NEt_3, DMF). Thus more concentrated reaction results in products that entrap more guest species leading to a faster decomposition upon heating. In contrast, the thermal stability of diluted reaction products (such as E_{160}) is approaching the thermal stability of conventional ZIF-8 compound.